

Effects of excess ammoniacal nitrogen ($\text{NH}_4^+ \text{-N}$) on pigments, photosynthetic rates, chloroplast ultrastructure, proteomics, formation of reactive oxygen species and enzymatic activity in submerged plant *Hydrilla verticillata* (L.f.) Royle

Danlu Shi^a, Kai Zhuang^a, Yahua Chen^{a,b}, Fuli Xu^c, Zhubing Hu^{d,*}, Zhenguo Shen^{a,b,**}

^a College of Life Sciences, Nanjing Agricultural University, Nanjing 210095, People's Republic of China

^b Jiangsu Collaborative Innovation Center for Solid Organic Waste Resource, Nanjing Agricultural University, Nanjing 210095, People's Republic of China

^c MOE Laboratory for Earth Surface Processes, College of Urban and Environmental Sciences, Peking University, Beijing 100871, People's Republic of China

^d Key Laboratory of Plant Stress Biology, School of Life Sciences, Henan University, Kaifeng 475004, People's Republic of China



ARTICLE INFO

Keywords:

Ammoniacal-nitrogen ($\text{NH}_4^+ \text{-N}$)
Proteomics
Carbon and nitrogen (C-N) metabolism
Chloroplast ultrastructure
Hydrilla verticillata (L.f.) Royle (*H. verticillata*)

ABSTRACT

Although excess ammoniacal-nitrogen ($\text{NH}_4^+ \text{-N}$) results in the disturbance of various important biochemical and physiological processes, a detailed study on the effects of $\text{NH}_4^+ \text{-N}$ stress on the photosynthesis and global changes in protein levels in submerged macrophytes is still lacking. Here, the changes of excess $\text{NH}_4^+ \text{-N}$ on physiological parameters in *Hydrilla verticillata* (L.f.) Royle, a submerged macrophyte were investigated, including the contents of photosynthetic pigments, soluble sugars, net photosynthesis and respiration, glutamine synthetase (GS) and glutamate synthase (GOGAT) activities, chloroplast ultrastructure, chloroplast reactive oxygen species (ROS) accumulation and protein levels. Our results showed that the net photosynthetic rate and pigment content reached maximum values when the plants were treated with 1 and 2 mg L⁻¹ $\text{NH}_4^+ \text{-N}$, respectively, and decreased at $\text{NH}_4^+ \text{-N}$ concentrations at 5, 10, 15 and 20 mg L⁻¹. This decrease might be caused by ROS accumulation. Compared that in 0.02 mg L⁻¹ $\text{NH}_4^+ \text{-N}$ as a control, ROS generation in chloroplasts significantly increased in the presence of more than 2 mg L⁻¹ $\text{NH}_4^+ \text{-N}$. Consistently, the damages caused by over-accumulated ROS were observed in chloroplast ultrastructure, showing a loose thylakoid membranes and swollen grana/stroma lamellae. Furthermore, through proteomic analysis, we identified 91 differentially expressed protein spots. Among them, six proteins involved in photosynthesis decreased in abundance in response to excess $\text{NH}_4^+ \text{-N}$. Surprisingly, the abundance of all the identified proteins that were involved in nitrogen assimilation and amino acid metabolism tended to increase under excess $\text{NH}_4^+ \text{-N}$ compared with the control, suggestive of the imbalanced carbon and nitrogen (C-N) metabolism. In support, activated GS and GOGAT cycle was observed, evidenced by higher activities of GS and GOGAT enzymes. To our knowledge, this work is the first description that excess $\text{NH}_4^+ \text{-N}$ results in chloroplast ultrastructural damages and the first proteomic evidence to support that excess $\text{NH}_4^+ \text{-N}$ can lead to a decline in photosynthesis and imbalance of C-N metabolism in submerged macrophytes.

1. Introduction

During the past several decades, the extensive applications of nitrogen (N) and phosphorus (P) fertilizers in modern agriculture have resulted in a severe environmental issue, which is eutrophication in freshwater lakes. Under eutrophication conditions, aquatic animals and plants are subjected to stresses, such as darkness and anoxia, which in turn threatened their survival (Bhagowati and Ahamed, 2019; Kautsky,

1991). In view of the crucial functions of aquatic plants in maintaining aquatic ecosystems, such as element cycles and oxygen production, it will be meaningful to dissect the mechanism of aquatic plants coping with eutrophication (Bakker et al., 2016; Bornette and Pujalon, 2011; Lewis and Pryor, 2013).

Hydrilla verticillata (L.f.) Royle is a perennial aquatic herb and can accumulate nitrogen, phosphorus and heavy metals by the uptake with both roots and leaves (He et al., 2016; Park et al., 2011; Wang et al.,

* Corresponding author.

** Corresponding author at: College of Life Sciences, Nanjing Agricultural University, Nanjing 210095, People's Republic of China.

E-mail addresses: zhubinghu@henu.edu.cn (Z. Hu), zgshen@njau.edu.cn (Z. Shen).

2010; Xue et al., 2010). Because of its capability of fast growth and high biomass yield, *H. verticillata* has been regarded as a high-potential plant for use in the remediation of contaminated aquatic ecosystems (Abu Bakar et al., 2013; Jain and Kalamdhad, 2018; Srivastava et al., 2010; Srivastava and D'Souza, 2009; Zhang and Liu, 2011). In view of the role and potential value of *H. verticillata*, an increasing effort has been devoted to understand its physiological and biochemical properties, when challenged with various stresses (Cao et al., 2004; Panda and Khan, 2004; Srivastava et al., 2006; Wang et al., 2010). However, its mechanisms of accumulation and tolerance to excess ammoniacal-nitrogen ($\text{NH}_4^+ \text{-N}$) are poorly understood.

Generally, in anoxic aquatic environments with high decomposition of organic matter or with high nitrogen-containing compound input, $\text{NH}_4^+ \text{-N}$ becomes a major factor contributing to the eutrophication (Saunkaew et al., 2011; Weisse, 2008). Jiang and Shen (2007) monitored water quality in Lake Donghu for one year and found the $\text{NH}_4^+ \text{-N}$ reached 0.96–30.48 mg L⁻¹ in January and February. Similar high nitrogen occurred in other waters in China, including Lixia river and Lake Taihu (Ma et al., 2015; Chen et al., 2009). Thus, understanding the effects of $\text{NH}_4^+ \text{-N}$ on submerged plants will definitely help us to cope with eutrophication problem.

$\text{NH}_4^+ \text{-N}$ is the predominant form of inorganic nitrogen taken up by plants (Bai et al., 2014; Zhou et al., 2015). As an essential macronutrient, nitrogen is involved in all of the biochemical and physiological processes, which control plant growth and development. However, excess $\text{NH}_4^+ \text{-N}$ disturbs cellular pH, ionic balance, ROS homeostasis and, thereby interfering with photosynthesis, membrane integrity, metabolisms of carbon and nitrogen (C-N) and mineral uptake (Britto and Kronzucker, 2002; Cao et al., 2004; Saunkaew et al., 2011; Zhong et al., 2013; Zhou et al., 2017). For instance, excess $\text{NH}_4^+ \text{-N}$ promotes the ROS production, such as superoxide anion (O_2^-) and hydrogen peroxide (H_2O_2) (Wang et al., 2010; Yin et al., 2016). Our previous study demonstrated that, under $\text{NH}_4^+ \text{-N}$ stress, O_2^- and H_2O_2 are mainly accumulated in the inner side of the plasma membrane and extracellular space of the mesophyll cells of *H. verticillata*, although O_2^- accumulation is also observed in chloroplasts (Zhuang et al., 2019). Further analysis demonstrated that the increased ROS might be attributed to the disturbance of excess $\text{NH}_4^+ \text{-N}$ on photosynthetic electron chain, and also on plasma membrane-bound nicotinamide adenine dinucleotide phosphate (NADPH) oxidase.

It is well-known that a number of genetic systems become activated by rapidly optimizing gene expression and protein production when plants suffered from stresses (Hazen et al., 2003; Kosová et al., 2011). High-resolution approaches, such as proteomics, have been widely employed to dissect the underlying molecular mechanisms and physiological changes in plants in response to various stresses (Jorrín et al., 2006; Rodziewicz et al., 2014). Not surprisingly, increasing number of reports can be found in studies of aquatic plants by using proteomics to investigate their physiological responses to abiotic stresses, including heavy metals (Kaszycki et al., 2018; Larras et al., 2013; Shi et al., 2017), nutrient conditions (Huang et al., 2014; Li et al., 2015; Longworth et al., 2016) and salinity (Thagela et al., 2017). However, no proteomics-based report has been published, yet, on $\text{NH}_4^+ \text{-N}$ -induced alterations in aquatic plants.

In the present study, experiments were conducted (1) to assess the effects of excess $\text{NH}_4^+ \text{-N}$ on photosynthesis in *H. verticillata*, by determining the net photosynthetic rate, chlorophyll content and chloroplast structure; (2) to understand the responses of *H. verticillata* to excess $\text{NH}_4^+ \text{-N}$ by analyzing the changes in protein abundance between $\text{NH}_4^+ \text{-N}$ stress and control conditions with a proteomic approach. We expected that $\text{NH}_4^+ \text{-N}$ stress will definitely disturb the photosynthesis. Meanwhile, *H. verticillata* will activate various mechanisms to repair or counteract the damages through altering protein abundance. Similar observations were reported in other studies by proteomics-based approaches (Huang et al., 2014; Longworth et al., 2016; Shi et al., 2017).

2. Materials and methods

2.1. Plant materials and growth conditions

The *H. verticillata* plants and growth condition were described previously (Shi et al., 2017). Subsequently, the 15 cm stem tips of the *H. verticillata* were treated with 5% Hoagland's nutrient solution supplemented with normal (0.02 mg L⁻¹ NH_4Cl as a control) and excess of $\text{NH}_4^+ \text{-N}$ (0.2, 1, 2, 5, 10, 15 and 20 mg L⁻¹) with three replications of containers for 5 days. For determination of O_2^- and H_2O_2 in the chloroplasts, observation of ultrastructure changes in leaves and proteomics analysis, only that plants under control, 0.2, 2 and 20 mg L⁻¹ excess $\text{NH}_4^+ \text{-N}$ treatment were used.

2.2. Measurement of the rates of net photosynthesis and respiration

The liquid-phase oxygen measurement system (Oxygraph, Hansatech UK) was used to determine the rates of net photosynthesis and respiration by following Lin's experimental procedure (Lin et al., 2009). The photosynthetic rate was assayed in growth medium supplemented with 10 mM NaHCO_3 under the light (100 $\mu\text{mol m}^{-2} \text{s}^{-1}$), while the respiration rate was measured under the darkness.

2.3. Determination of photosynthetic pigments, soluble sugars, soluble proteins, glutamine synthetase and glutamate synthase activities in shoots

Photosynthetic pigments in shoots of *H. verticillata* (0.10 g fresh tips with surface blotted dry) were extracted with 95% ethanol in the dark for 12 h. Subsequently, the optical density (OD_{665} , OD_{649} and OD_{470} nm) was measured. The contents of photosynthetic pigments were calculated according to the formulas described previously (Kautsky, 1991).

The content of soluble sugars was determined by the anthrone-sulfuric acid method (Yemm and Willis, 1954) and soluble proteins were determined using Coomassie brilliant blue G-250 (Bradford, 1976).

The extraction of glutamine synthetase (GS) was carried out with Tris-HCl buffer (50 mM, pH 8.0, 2 mM EDTA, 20 mM 2-mercaptoethanol, and 1 mM phenylmethylsulfonyl fluoride). The extraction of glutamate synthase (GOGAT) was carried out with sodium phosphate buffer (200 mM, pH 7.5, 2 mM EDTA, 50 mM KCl, 0.1% (v/v) β -mercaptoethanol and 0.5% (w/v) Triton X-100). GS activity was determined by the hydroxamate biosynthetic method (Berteli et al., 1995) and GOGAT activity was determined by evaluating the NADH oxidation rate (Singh et al., 1986).

2.4. Determination of O_2^- and H_2O_2 in the chloroplasts

Eighty gram fresh weight of *H. verticillata* were used to isolate chloroplasts by horizontal centrifugation with Percoll cell separation solution as described previously (Kieselbach et al., 1998; Marmagne et al., 2006). Chloroplasts with the membrane integrity over 90% were used in subsequent experiments (Table 1), which were checked with liquid-phase oxygen measurement system.

The production of O_2^- by chloroplasts was measured by the NBT method according to Navari-izzo et al. (1999). Simply, after irradiating

Table 1

The rates of O_2 release of intact/lysed chloroplasts, and percentage of intact chloroplasts after purification.

	Control	0.20 Concentration of $\text{NH}_4^+ \text{-N}$, mg L ⁻¹	2.00	20.00
Intact chloroplasts ($\mu\text{mol O}_2 \text{ mg}^{-1} \text{ Chl h}^{-1}$)	7.6 ± 0.3	7.2 ± 0.7	6.5 ± 0.5	4.5 ± 0.8
Lysed chloroplasts ($\mu\text{mol O}_2 \text{ mg}^{-1} \text{ Chl h}^{-1}$)	7.6 ± 0.3	7.6 ± 0.3	7.6 ± 0.3	7.6 ± 0.3
Percentage (%)	94.7	90.9	92.7	92.6

the reaction solution under an 150 W fluorescent lamp for 10 min, the OD₅₆₀ value was determined. Thiocarbamate was used as superoxide dismutase (SOD) activity inhibitor. The H₂O₂ content was determined by trichloroacetic acid (TCA) and potassium iodide (KI) method (Loreto and Velikova, 2001). The H₂O₂ content was calculated based on a standard curve previously made by using different concentrations of H₂O₂.

2.5. Observation of ultrastructure changes in leaves and proteomics analysis

Ultrastructural changes in leaves were observed with transmission electron microscope (TEM) performed according to the method of Molas (1998).

Proteomics studies were carried out following the approach described in our previous study with three independent replicates (Shi et al., 2017). Proteins were extracted by an improved trichloroacetic acid/acetone method and protein concentration was determined using the modified Bradford assay, with ovalbumin as the standard. For isoelectric focusing, 100 µg of total proteins and pH 4–7 linear gradient dry strips (17 cm; Bio-Rad, USA) were used, and a 12% SDS-polyacrylamide gels were approached in second dimension electrophoresis. The resulting gel was imaged by mass spectrometry-compatible silver staining and acquired at 300 dpi resolution. Data analysis was performed using PD Quest software (Version 8.0; Bio-Rad). Protein spots were selected for MS analysis when a difference of 1.5-fold or greater was observed in the level of accumulation between the treatment and control. Protein spots were excised, de-stained, and analyzed using a MALDI-TOF mass spectrometer (Reflex III; Bruker-Daltonics) in the reflection/delayed extraction mode. Calibration was carried out using a standard peptide mixture. MS data was collected from mono-isotopic peaks in the mass range 500–3000 Da with a signal/noise ratio > 10. MaxQuant (Version 1.5.2.5) was used to search the local transcriptome database of *H. verticillata*.

2.6. Statistical Analysis

Data were statistically analyzed in SPSS version 20.0. The distribution of the data is normal when analyzed with the One-Sample Kolmogorov-Smirnov test method. And variances of the data showed the homogeneous distribution when tested by Levene's method. Then the data were analyzed by ANOVA statistical test. Tukey's HSD tests (at P < 0.05) were used for significant difference between groups. The graphs were generated by GraphPad Prism 5.

3. Results

3.1. Effects of NH₄⁺-N on net photosynthetic and respiration rates, and soluble sugar content

Compared with the control, five-day treatments with excess NH₄⁺-N (0.2, 1 and 2 mg L⁻¹) significantly increased the net photosynthesis rate, determined by the rate of O₂ release, in shoots (Fig. 1A). The highest rate of O₂ release was present in the treatment with 1 mg L⁻¹ NH₄⁺-N. For NH₄⁺-N concentrations above 1 mg L⁻¹, the O₂ release rate decreased significantly. In contrast, the respiration rate, measured by the rate of O₂ consumption, increased almost linearly with the increase of NH₄⁺-N in solution (Fig. 1B). As plant photosynthesis is a process that requires cells to use carbon dioxide and energy from the light to generate sugar molecules and oxygen, we also evaluated the changes in soluble sugars in shoots and found that the content of soluble sugars peaked at 1 mg L⁻¹ NH₄⁺-N (Fig. 1C).

3.2. Effects of NH₄⁺-N on pigment contents and chloroplast structure

As pigments are the key components to absorb light energy to produce sugar, we firstly measured the contents of different pigments

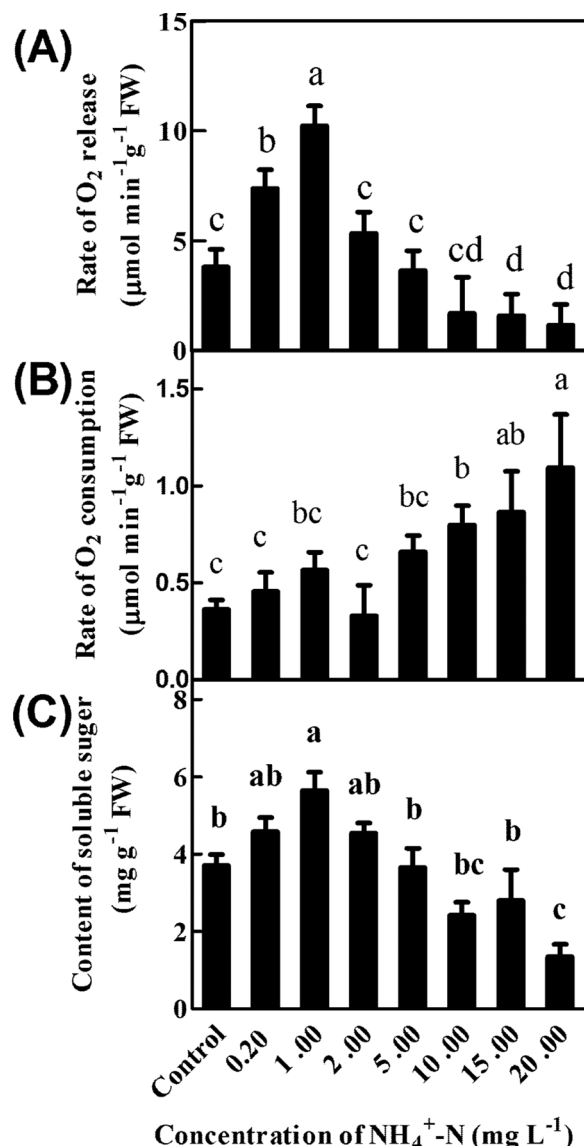


Fig. 1. The rates of net photosynthesis (A), respiration (B) and soluble sugar content (C) of *H. verticillata* shoots exposed to different concentrations of NH₄⁺-N for 5 days. For each parameter, different letters indicate significant difference among treatments according to Tukey's HSD test (p < 0.05). Each bar indicates the mean ± standard deviation (n = 3).

under various NH₄⁺-N treatments. As shown in Fig. 2, when compared with the control, the presence of 1 and 2 mg L⁻¹ NH₄⁺-N in the treatment solution significantly increased the contents of chlorophyll *a* (chl_a) and carotene, as well as the ratio of the chl_a/chl_b (Fig. 2A, C and D). NH₄⁺-N treatments did not significantly affect the content of chl_b until more than 10 mg L⁻¹ had been applied (Fig. 2B). The highest contents of chl_a, chl_b and carotene, as well as the highest ratio of chl_a/chl_b were observed in the treatment of 2 mg L⁻¹ NH₄⁺-N. A significant decrease in chl_a occurred when NH₄⁺-N concentrations were above 10 mg L⁻¹, while NH₄⁺-N higher than over 15 mg L⁻¹ resulted in a significant reduction in chl_b levels.

As pigments are localized in chloroplast and crucial for photosynthesis, we next investigated the effects of NH₄⁺-N on chloroplast ultrastructure with 0.2, 2 and 20 mg L⁻¹ NH₄⁺-N. In the control and 0.2 mg L⁻¹ NH₄⁺-N treatment, an abundant well-organized inner membrane system with dense thylakoid and parallel pattern of lamellae was found, and plentiful starch granules were accumulated in the chloroplasts (Fig. 3A and B). In contrast, some chloroplast thylakoid lamellae

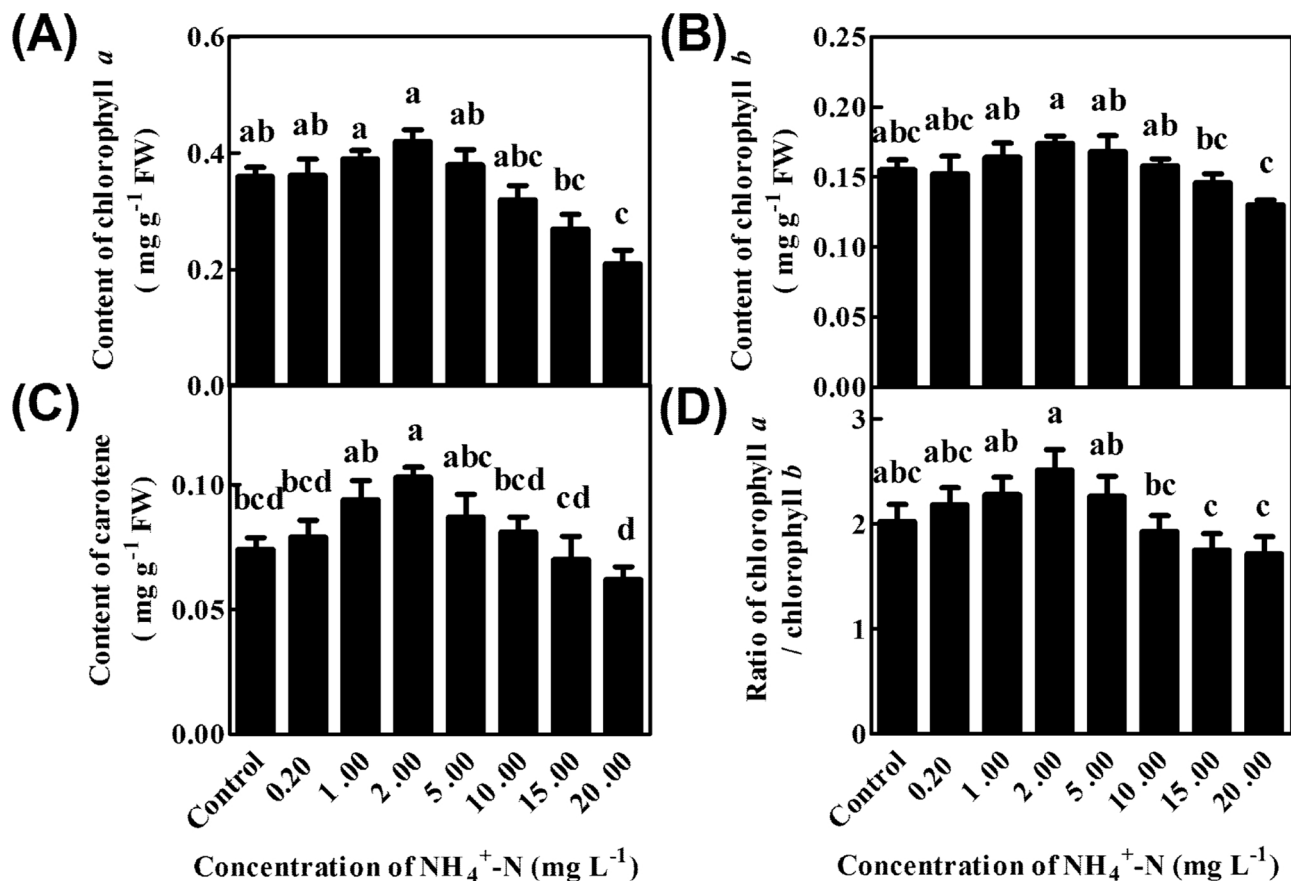


Fig. 2. Photosynthetic pigments contents in *H. verticillata* shoots exposed to different concentrations of $\text{NH}_4^+ \text{-N}$ for 5 days. A, content of chlorophyll *a*; B, content of chlorophyll *b*; C, content of carotene; D, ratio of chlorophyll *a* / chlorophyll *b*. For each parameter, different letters indicate significant difference among treatments according to Tukey's HSD test ($p < 0.05$). Each bar indicates the mean \pm standard deviation ($n = 3$).

showed swelling, thylakoid membrane distortion became apparent, and starch grains decreased or even disappeared in the treatment of $2 \text{ mg L}^{-1} \text{NH}_4^+ \text{-N}$ (Fig. 3C). The damage intensified when plants were exposed to $20 \text{ mg L}^{-1} \text{NH}_4^+ \text{-N}$. At this treatment, breakages in the chloroplast envelope occurred. High $\text{NH}_4^+ \text{-N}$ distorted the lamellae arrangement, loosened the thylakoid membranes and reduced the starch grains (Fig. 3D).

3.3. Effects of $\text{NH}_4^+ \text{-N}$ on $\text{O}_2^{\cdot-}$ and H_2O_2 accumulation in chloroplasts

When light energy is not efficiently transferred to chemical energy, superoxide anion ($\text{O}_2^{\cdot-}$) is generated during the electron transport chain of the chloroplast. To test whether $\text{NH}_4^+ \text{-N}$ stress leads to the increase of ROS production in *H. verticillata*, we determined the production rate of H_2O_2 and $\text{O}_2^{\cdot-}$ in chloroplasts under 0.2 , 2 and $20 \text{ mg L}^{-1} \text{NH}_4^+ \text{-N}$. Consistently with the disordered structure of chloroplast structure, the presence of 2 and $20 \text{ mg L}^{-1} \text{NH}_4^+ \text{-N}$ significantly induced H_2O_2 accumulation and $\text{O}_2^{\cdot-}$ production rate in chloroplasts, while no significant effect was observed upon the treatment of $0.2 \text{ mg L}^{-1} \text{NH}_4^+ \text{-N}$ (Fig. 4).

3.4. Identification of differentially expressed proteins

The above-mentioned results clearly demonstrated that $\text{NH}_4^+ \text{-N}$ stress dramatically influenced photosynthesis in *H. verticillata*. Next, we investigated the underlying molecular physiology under $\text{NH}_4^+ \text{-N}$ stress. We employed proteomics to compare the abundance of proteins in the presence and absence of $\text{NH}_4^+ \text{-N}$ stress. Total soluble proteins were obtained from the shoots treated with 0.2 , 2 and $20 \text{ mg L}^{-1} \text{NH}_4^+ \text{-N}$ for 5 days. Compared to the control (0.02 mg L^{-1}), the content of soluble

proteins was increased by low $\text{NH}_4^+ \text{-N}$ ($1\text{-}10 \text{ mg L}^{-1}$) but decreased by high $\text{NH}_4^+ \text{-N}$ ($15\text{-}20 \text{ mg L}^{-1}$). The highest contents of soluble proteins were observed after treatment with 2 and $5 \text{ mg L}^{-1} \text{NH}_4^+ \text{-N}$ (Fig. 5).

Next, the samples from the treatments of 0.02 (control), 0.2 , 2 and $20 \text{ mg L}^{-1} \text{NH}_4^+ \text{-N}$ were used for two-dimensional gel electrophoresis (2-DE). By using the silver-staining method, we detected reproducibly a total of 587 protein spots on three independent sheets of gel (Fig. 6 and Supplemental Fig. 1). Representative gels and five enlarged typical regions were shown in Figs. 6 and 7, respectively. According to quantitative image analysis, a total of 91 protein spots were found that showed more than 1.5-fold changes in abundance between control and at least one of three NH_4^+ -treatments. Compared with the control, the intensity of 48 protein spots tended upwards and 15 spots tended downwards in response to $\text{NH}_4^+ \text{-N}$ treatment. The intensity of three spots increased with low $\text{NH}_4^+ \text{-N}$ or unchanged but were down-regulated by high $\text{NH}_4^+ \text{-N}$ treatment. In contrast, 19 protein spots decreased or unchanged by low $\text{NH}_4^+ \text{-N}$ but increased by high $\text{NH}_4^+ \text{-N}$ treatment. In general, changes in spot intensity became more pronounced with increasing $\text{NH}_4^+ \text{-N}$ concentrations. Moreover, three spots were newly induced by $20 \text{ mg L}^{-1} \text{NH}_4^+ \text{-N}$ and not detected in other treatments.

The 91 differentially expressed protein spots were characterized by MALDI-TOF-MS (matrix-assisted laser desorption/ionization time-of-flight mass spectrometry) and identified by PMF (peptide mass fingerprinting). Among those protein spots, 53 showed homology with 52 known proteins after database search (Table 2), while the remaining 38 could not be identified. These 52 NH_4^+ -responsive proteins included those involved in photosynthesis (spots 3, 10, 13, 14, 16, 17, 19, 22, 23, 26, 38, 39, 46 and 49), carbohydrate metabolism (spots 9, 25, 27, 40, 41, 44, 45 and 48), nitrogen assimilation and amino acid metabolism

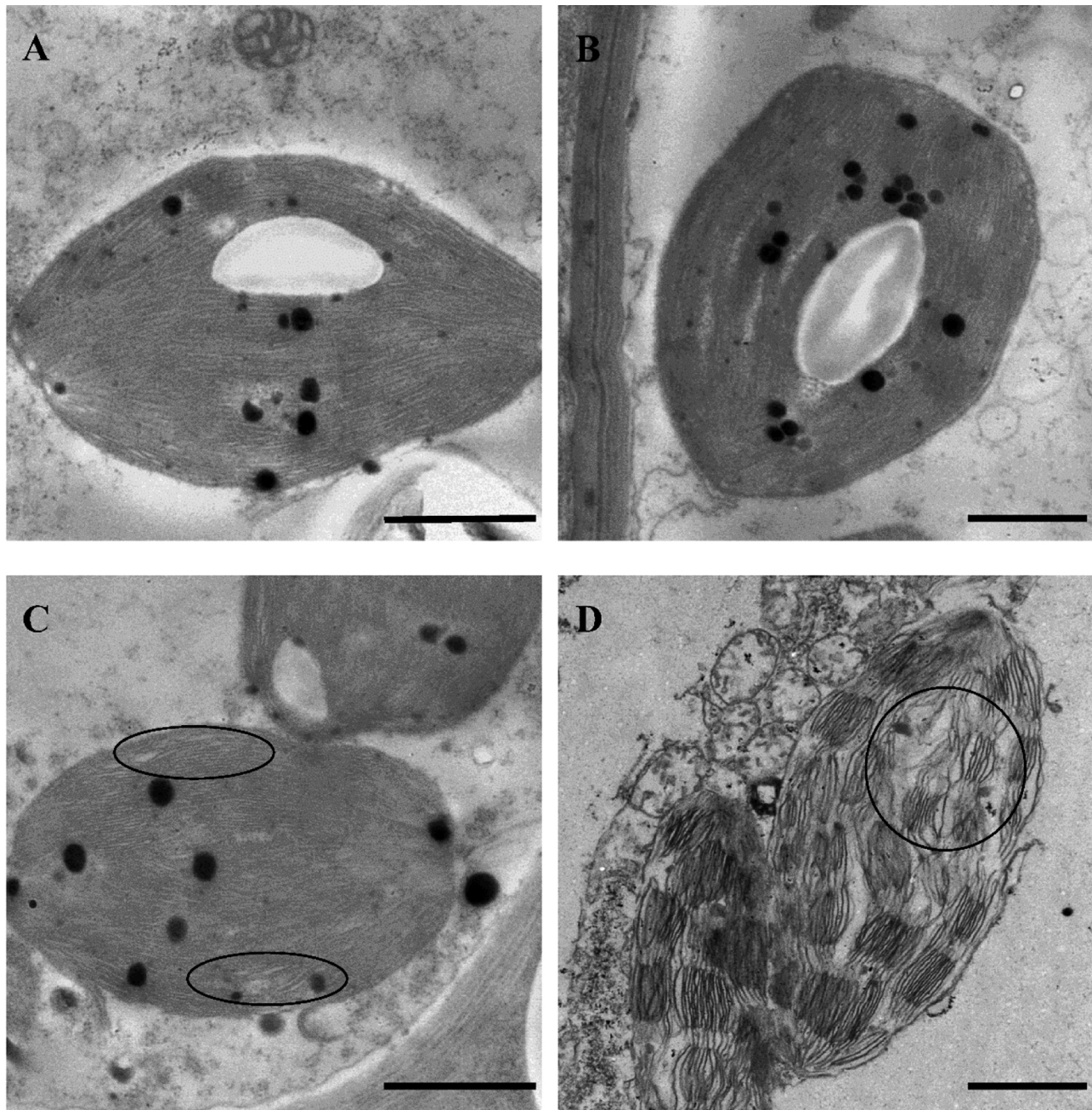


Fig. 3. Chloroplast structure changes in *H. verticillata* leaves exposed to different concentrations of $\text{NH}_4^+ \text{-N}$ for 5 days. A, Control plants; B, plants treated with $0.20 \text{ mg L}^{-1} \text{NH}_4^+ \text{-N}$; C, plants treated with $2.00 \text{ mg L}^{-1} \text{NH}_4^+ \text{-N}$; D, plants treated with $20.0 \text{ mg L}^{-1} \text{NH}_4^+ \text{-N}$. All plants were treated for 5 days, then subjected to TEM observations. Bars represent $1.0 \mu\text{m}$.

(spots 11, 12, 15, 24, 28, 34, 35 and 50), transcription regulation (spots 18 and 31), protein folding and hydrolysis (spots 1, 2, 4, 5, 6, 7, 8, 21, 32, 36 and 47), antioxidative defense and redox regulation (spots 30, 33, 37, 42, 43, 52 and 53), and some proteins with other various functions (spots 20, 29 and 51). It is interesting to notice that six proteins (spots 3, 10, 13, 17, 23 and 46) showing a decreased abundance in response to high $\text{NH}_4^+ \text{-N}$ treatment were identified as those involved in photosynthesis. In contrast, the abundance of proteins involved in carbohydrate metabolism, as well as nitrogen assimilation and amino acid metabolism, tended to increase under $\text{NH}_4^+ \text{-N}$ treatment compared with the control, suggesting an imbalance of carbon and nitrogen metabolisms under $\text{NH}_4^+ \text{-N}$ stress.

3.5. Effects of $\text{NH}_4^+ \text{-N}$ on the activities of GS and GOGAT

Plant cells are able to incorporate $\text{NH}_4^+ \text{-N}$ into glutamine to produce glutamate. This process requires two important enzymes, GS and GOGAT, named the GS-GOGAT cycle, by which a carbon skeleton is provided for nitrogen assimilation. Thus, the GS-GOGAT cycle plays a key roles in maintaining the balance of carbon and nitrogen. We measured the activity of GS and GOGAT in *H. verticillata* under 0.02 (Control), 0.20 , 1.00 , 2.00 , 5.00 , 10.00 , 15.00 and $20.00 \text{ mg L}^{-1} \text{NH}_4^+ \text{-N}$ treatments. No significant change in the activity of GS and GOGAT in shoots occurred in the treatments with 0.2 and $1 \text{ mg L}^{-1} \text{NH}_4^+ \text{-N}$ in comparison with the control (Fig. 8). However, with increasing $\text{NH}_4^+ \text{-N}$ level from 2 mg L^{-1} onwards, the activities of GS and GOGAT increased

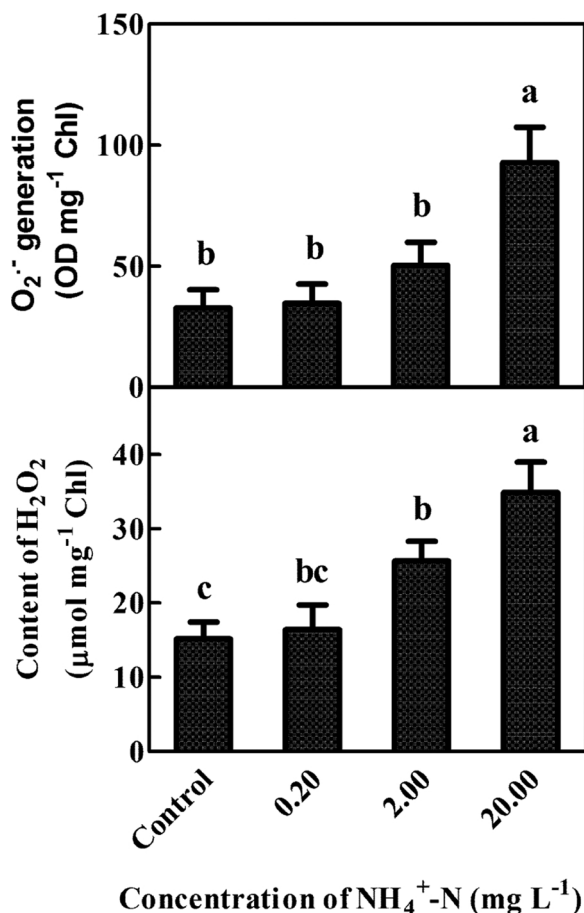


Fig. 4. Formation of O₂⁻ and H₂O₂ in *H. verticillata* shoots exposed to different concentrations of NH₄⁺-N for 5 days. (A) generation of O₂⁻ in the chloroplasts of *H. verticillata* leaves; (B) content of H₂O₂ in the chloroplasts of *H. verticillata* leaves. For each parameter, different letters indicate significant difference among treatments according to Tukey's HSD test ($p < 0.05$). Each bar indicates the mean \pm standard deviation ($n = 3$).

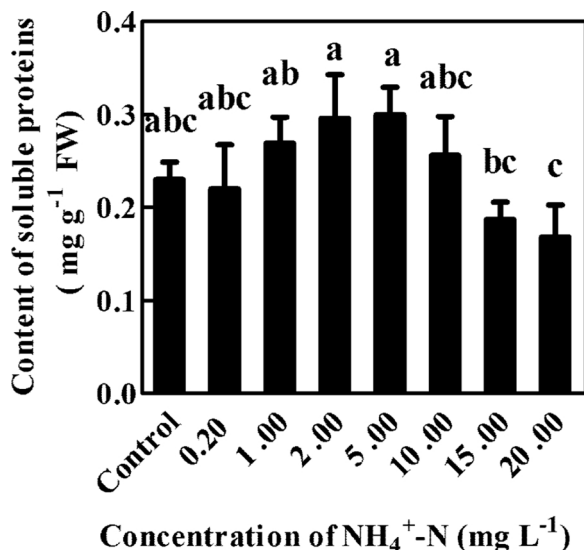


Fig. 5. Soluble protein contents in *H. verticillata* shoots exposed to different concentrations of NH₄⁺-N for 5 days. For each parameter, different letters indicate significant difference among treatments according to Tukey's HSD test ($p < 0.05$). Each bar indicates the mean \pm standard deviation ($n = 3$).

(Fig. 8A and B), further supporting a disturbed balance of carbon and nitrogen metabolisms.

4. Discussion

Higher plants take up nitrogen for their growth and development in the forms of NO₃⁻ (NO₃-N) and NH₄⁺ (NH₄⁺-N). At low levels, NH₄⁺-N is a preferred N form for most aquatic macrophytes, while at high levels, it can cause toxicity symptoms in plants (Britto and Kronzucker, 2002). Excess NH₄⁺-N can disturb nutrient uptake, decrease chlorophyll content and photosynthesis rate, induce oxidative stress and cause internal carbon-nitrogen imbalance (Apudo et al., 2016; Wang et al., 2010; Su et al., 2012; Yin et al., 2016; Zhong et al., 2013). In this study, low NH₄⁺-N tended to increase the contents of chla, chlb and carotene, but at 5 mg L⁻¹ NH₄⁺-N and above, there was a decline in the contents of these pigments compared to levels obtained at 2 mg L⁻¹ NH₄⁺-N. In accordance with this, Wang et al. (2010) observed that the content of total chlorophyll decreased by about 18%, 28% and 44%, respectively, after treatment with 0.5, 1.5 and 3 mM NH₄Cl (equivalent to 7, 21 and 42 mg L⁻¹ NH₄⁺-N) for 4 days compared with the control (0 mg L⁻¹ NH₄⁺-N) in *H. verticillata*. In other aquatic plant species (*Myriophyllum spicatum*), five-day treatment with 50 mg L⁻¹ NH₄⁺-N significantly decreased the chlorophyll content (Apudo et al., 2016). The 2 and 8 mg L⁻¹ NH₄⁺-N treatments resulted in leaf chlorosis in submersed macrophytes *M. spicatum* and *Ceratophyllum demersum*, respectively (Zhong et al., 2013). Many variables influence the toxicity of excess NH₄⁺-N, such as plant species, duration of treatment and the experimental conditions. For example, Su et al. (2012) observed that five-day treatment with 30 mg L⁻¹ NH₄⁺-N had no significant effect on the total chlorophyll content in apical shoots of submersed macrophyte, *Egeria densa*, but significantly increased lipid peroxidation, as indicated by malondialdehyde content. Similarly, Yin et al. (2016) reported that 15-day treatment with 10 mg L⁻¹ NH₄⁺-N only led to a slight decrease of the chlorophyll synthesis of submersed macrophyte, *Potamogeton crispus*, but that NH₄⁺-N concentrations ≥ 4 mg L⁻¹ significantly increased MDA content and ROS production.

It has been proposed that NH₄⁺-N can inhibit the synthesis of pigments by suppressing uptake of minerals (Britto and Kronzucker, 2002) and/or increasing their degradation by inducing production of ROS (Gomes et al., 2016; Wang et al., 2010; Wang et al., 2015; Zaefyzadeh et al., 2009). The H₂O₂ content in *H. verticillata* treated with 0.5 mM NH₄Cl for 12 h increased significantly when compared with the control, while the chlorophyll and carotenoid contents did not decrease in these plants (Wang et al., 2010). In our previous study, O₂⁻ dependent DAB precipitates were observed in the chloroplasts (Zhuang et al., 2019). This suggest that the decline in synthetic pigments may be attributed, at least in part, to NH₄⁺-induced oxidative stress. Further studies should be conducted to investigate the possible link between the concentrations of photosynthetic pigments and ROS production under NH₄⁺-N stress.

Although there are many reports concerning decreased photosynthetic pigment contents in response to excess NH₄⁺-N, relatively little information is available about photosynthetic rate alterations in aquatic macrophytes under NH₄⁺-N stress. Piwpuan et al. (2014) observed that the photosynthetic rate in *Actinoscirpus grossus* did not differ significantly among treatments with 0.5–15 mM NH₄⁺-N. Under our experimental conditions, *H. verticillata* was able to grow well in water with excess NH₄⁺-N up to 5 mg L⁻¹, and the net photosynthetic rate and contents of chla, chlb and carotene reached their maximum values when the plants were treated with 1 and 2 mg L⁻¹ NH₄⁺-N, respectively. However, at concentrations ≥ 10 mg L⁻¹, the net photosynthetic rate and chlorophyll a content were significantly lower than those in the control (0.02 mg L⁻¹ NH₄⁺-N). Our results suggest that net photosynthetic rate may be more sensitive than pigment content in response to NH₄⁺-N stress.

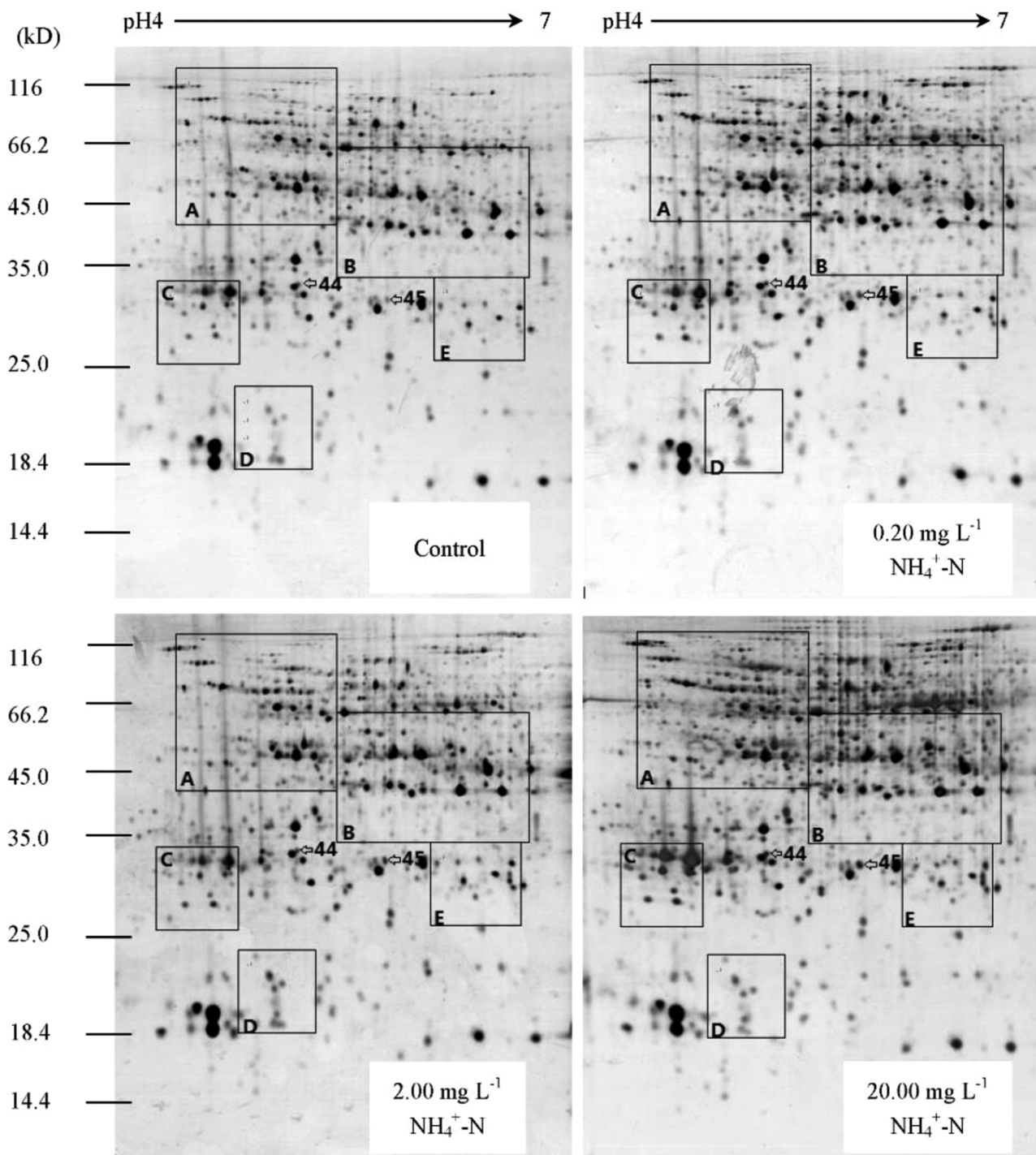


Fig. 6. Separation of the total proteins extracted from the shoots of the *H. verticillata* on two-dimensional electrophoresis gels over the pH range 4–7. The Materials were treated with 0.02 (Control), 0.20, 2.00 and 20.00 mg L⁻¹ NH₄⁺-N (NH₄Cl) for 5 days. The 53 differentially expressed proteins are marked. The framed regions are enlarged in Fig. 7. The protein spots are numbered and correspond to the numbers in Table 2.

toxicity, evidenced by the changes in net photosynthetic rate and the significant decline in the content of soluble sugars at $\geq 2 \text{ mg L}^{-1}$ NH₄⁺-N when compared to that obtained at 1 mg L^{-1} NH₄⁺-N. Previous studies showed that 3 mg L^{-1} NH₄⁺-N decreased the soluble carbohydrate content in leaves and stems of 11 submersed macrophytes, including *H. verticillata* (Yuan et al., 2013). The decreased soluble sugars may be attributed to the consumption of C-skeletons and energy required for free amino acids (FAA) synthesis. Accumulation of FAA and decrease of soluble carbohydrates were found in some aquatic macrophytes under high NH₄⁺-N treatment (Cao et al., 2004; Dou et al., 2013; Yuan et al.,

2017; Yuan et al., 2015). Moreover, plant cells actively export NH₄⁺ as a mechanism of NH₄⁺ detoxification, which is an energy requiring process. Exporting NH₄⁺ resulted in a 40% increase in root respiration in a NH₄⁺-sensitive barley (Britto et al., 2001). Our results showed that the respiration rate increased substantially with increasing NH₄⁺-N concentration, which may reflects the higher availability of tricarboxylic acid cycle intermediates and energy for avoiding NH₄⁺-N accumulation in plant cells.

The chloroplast is the core component during the photosynthesis and is highly sensitive to environmental stresses. In terrestrial plants

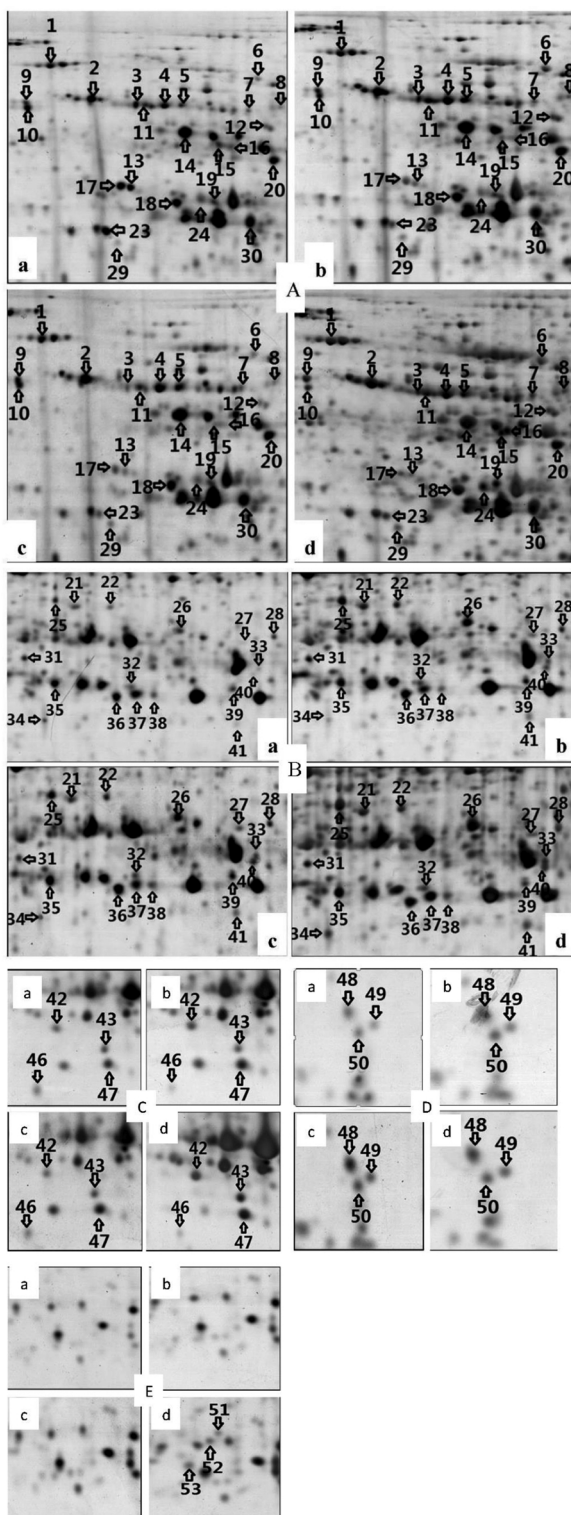


Fig. 7. Enlargements of the framed areas shown in Fig. 6. The framed regions A, B C, D and E in Fig. 6 are enlarged and compared in detail. a: Control; b: 0.20 mg L⁻¹ NH₄⁺-N; c: 2.00 mg L⁻¹ NH₄⁺-N; d: 20.00 mg L⁻¹ NH₄⁺-N.

treated with high levels of NH₄⁺-N, altered shape chloroplasts, swollen grana compartments with expanded loculi, and grana and stroma lamellae squeezed and destroyed by large starch granules were observed (Dou et al., 2013; Puritch and Barker, 1967). However, there is a lack of information on changes in the chloroplast ultrastructure of aquatic macrophytes under excess NH₄⁺-N. In the present study, we observed that alterations in chloroplast ultrastructure occurred in *H. verticillata*

leaves treated with 2 mg L⁻¹ NH₄⁺-N, which resulted in a significant decrease in the net photosynthetic rate compared with 1 mg L⁻¹ NH₄⁺-N treatment. The damage in chloroplast structure might provide the primary explanation for the decrease in photosynthesis rate of *H. verticillata*. Accumulation of ROS in chloroplasts may lead to damaged chloroplast ultrastructure.

Relatively few proteomic-based studies have been conducted on the responses of aquatic macrophytes to excess NH₄⁺-N. In this study, fourteen proteins involved in photosynthesis were identified. The abundance of six proteins decreased, while eight proteins increased under high NH₄⁺-N treatment, indicating high NH₄⁺-N disturbed the photosynthesis. For an instance, Spot 46 was identified as a light-harvesting chlorophyll a/b proteins (LHCPS) precursor. LHCPS, which are embedded in the thylakoid membrane, can bind different auxiliary pigments or antenna pigments to capture and transfer light energy in the chloroplast. Thus, the amount of LHCPS directly affects the efficiency of photosynthesis (Horn et al., 2007; Horn and Paulsen, 2002). Reduced expression of these proteins showed that high levels of NH₄⁺-N may inhibit LHCPS protein synthesis, leading to reduced capture of light. The decrease in the expression of these proteins might be a way to compensate for the oxidative stress caused by the excess of NH₄⁺-N, since with less chlorophylls available in the thylakoid, less electrons pass through the transport chain and, consequently, less stress is caused. Furthermore, protein spots 19 and 13 were identified as OEE 1 and OEE 2, respectively. Excess NH₄⁺-N treatment decreased the expression of OEE 2 but increased the expression of OEE 1. Oxygen-evolving enhancer protein (OEE) is polymerized by OEE 1, 2, and 3, which is related to the oxygen release during photosynthesis. OEE is located on the chloroplast thylakoid membrane, closely integrated with PS II, and helps PS II release O₂ (Heide et al., 2004; Yamamoto et al., 1988). Mayfield et al. (1987) found that the expression of OEE 2 depended on the high oxygen release efficiency of the PS II system, and the OEE 2 expression was down-regulated in a chloroplast with low oxygen release efficiency. The reduced OEE 2 expression may be related to the inhibited photosynthetic oxygen release rate. Some studies have found that OEE 1 has antioxidant activity, which can remove excess H₂O₂ directly (Heide et al., 2004; Kim et al., 2015). Therefore, it is possible that accumulation of ROS in the chloroplast could induce the up-regulation of OEE 1 under NH₄⁺-N stress.

Spots 3 and 23 were identified as putative transketolase (TK) and phosphoribulokinase (PRK), respectively. They showed a decrease in abundance after NH₄⁺-N treatments. In the Calvin cycle, transketolase and aldolase enzymes catalyze a series of changes, namely the conversion of fructose-6-phosphate, 3-phosphate-glyceraldehyde and sedoheptulose 7-phosphate into ribulose 5-phosphate, which is further phosphorylated to RuBP by PRK (Wilson and Calvin, 1955). Henkes et al. (2001) found that lowering TK activity strongly inhibited the recycle of ribulose-1,5-bisphosphate, thereby decreased the rate of photosynthesis. Banks et al. (1999) found that the effects of PRK activity on photosynthesis and growth was dependent on the levels of N supply in transgenic tobacco. In fact, the decrease of TK and PRK expression or activity can significantly affect plant photosynthesis.

Spot 17 was identified as predicted GSA-AT (predicted: glutamate-1-semialdehyde 2,1-aminomutase, chloroplastic-like). The GSA-AT is the sole producer of 8-aminolevulinic acid (ALA) for chlorophyll synthesis, and the synthetic process of ALA consumes NH₄⁺-N in chloroplast (Gough et al., 1993; Stenbaek and Jensen, 2010). Excess NH₄⁺-N treatment inhibited the GSA-AT expression, which might block the chlorophyll biosynthesis and can cause an accumulation of NH₄⁺ ions in the chloroplasts.

Carbon and nitrogen metabolisms are two important biochemical and physiological processes for the growth and development of all plants. To protect themselves from NH₄⁺-N toxicity, several mechanisms have been developed to keep high assimilation rates of inorganic nitrogen into FAA and amines, or to actively transport NH₄⁺-ions out of plant cells (Britto and Kronzucker, 2002). This process of FAA

Table 2
Identification of the differentially expressed proteins in the shoots of two *H. verticillata* in response to NH_4^+ -N stress by PMF (peptide mass fingerprinting).

Spot ID	Protein name	Fold-change	Concentration of NH_4^+ -N (mg L^{-1})	Score Mr/PI				Organism	Accession No.		
				Experimental		Theoretical					
				SC (%)	M	SC (%)	M				
Proteins involved in photosynthesis											
3	Putative transketolase	0.9	0.12↓	0.32↓	36.36	6	120	70.4/4.75	80.5/6.12		
23	Phosphoribulokinase	0.77	0.73	0.42↓	24.39	5	274	43.9/4.69	46.1/5.75		
13	Oxygen-evolving enhancer protein 2	0.32↓	0.21↓	0.11↓	30.16	3	89	45.2/4.75	28.3/8.29		
10	ATP synthase Cf 1 alpha subunit (chloroplast)	0.83	1.03	0.43↓	24.48	7	176	55.2/5.49	29.7/8.65		
14	ATP synthase Cf 1 beta subunit (chloroplast)	1.24	1.31	1.68↑	45.61	5	93	42.1/4.72	52.0/5.27		
19	PREDICTED: oxygen-evolving enhancer protein 1, chloroplastic ribulose-1,5-bisphosphate carboxylase/oxygenase large subunit	0.96	0.87	2.18↑	25.96	4	214	44.9/5.02	35.05/5.57		
22	ribulose-1,5-bisphosphate carboxylase/oxygenase large subunit	2.31↑	2.05↑	2.64↑	45.32	3	96	53.2/5.89	52.8/5.96		
26	ribulose-1,5-bisphosphate carboxylase/oxygenase large subunit	3.23↑	2.46↑	5.78↑	22.38	2	116	54.3/6.12	52.8/5.96		
Proteins involved in photosynthesis											
38	Photosystem II stability/assembly factor, chloroplast (HCF 136) isoform 1	0.2↓	1.32	1.52↑	23.99	4	164	44.1/6.03	45.1/7.76		
46	light-harvesting chlorophyll a/b protein precursor	0.43↓	0.98	0.32↓	32.32	16	92	27.6/4.28	28.3/5.16		
39	PREDICTED: ferredoxin-NADP reductase, leaf isozyme, chloroplastic Ferredoxin-NADP reductase, leaf isozyme, chloroplastic putative: ferredoxin-NADPH oxidoreductase (FNR)	1.72↑	1.86↑	1.43↓	51.38	7	172	45.1/6.45	41.1/8.51		
49	1.31	1.56↑	1.63↓	43.48	3	83	19.9/5.01	27.6/5.38			
16	PREDICTED: glutamate-1-semialdehyde 2,1-aminomutase, chloroplastic-like	0.86	0.13↓	2.36↓	17.03	1	97	49.6/5.19	40.4/6.92		
17	PREDICTED: glutamate-1-semialdehyde 2,1-aminomutase, chloroplastic-like	0.41↓	0.21↓	0.11↓	30.43	1	335	45.6/4.75	50.2/5.77		
Proteins involved in C metabolism											
9	PREDICTED: 2,3-bisphosphoglycerate-independent phosphoglycerate mutase	1.21	1.28	1.76↑	34.06	9	231	60.5/4.35	60.5/5.31		
25	Dihydrolipoyle dehydrogenase 1	2.25↑	2.03↑	4.23↑	71.43	3	268	56.2/5.63	52.7/6.90		
27	PREDICTED: biotin carboxylase 2, chloroplastic	0.96	1.57↑	1.32	49.47	5	189	53.2/6.68	58.3/6.85		
40	PREDICTED: endopeptidase isoform XI	2.36↑	3.60↑	3.76↑	45.12	5	114	46.3/6.61	47.0/7.20		
41	Glyceraldehyde-3-phosphate dehydrogenase 1, cytosolic	1.67↑	1.73↑	2.31↑	34.12	6	67	36.1/6.57	36.5/6.67		
44	cytosolic NAD-malate dehydrogenase	1.43	1.32	1.67↑	26.58	1	368	32.6/5.09	34.6/4.91		
45	fructose-1,6-bisphosphatase	1.42	1.65↑	2.03↑	39.06	11	265	30.1/5.76	35.9/6.25		
48	glyceraldehyde-3-phosphate dehydrogenase	1.47	1.69↑	1.58↑	31.3	10	283	21.4/4.72	24.01/5.64		
Proteins involved in N anabolism											
11	glutamine synthetase	2.75↑	1.23	1.60↑	27.32	17	312	69.8/6.72	80.4/5.90		
12	PREDICTED: glutathione synthetase, chloroplastic-like isoform X1	1.67↑	0.86	1.78↑	45.10	6	67	58.9/5.19	60.2/6.02		
15	PREDICTED: 5-methyltetrahydropteroylglutamate-homocysteine methyltransferase 1	0.34↓	0.13↓	1.89↓	21.53	6	126	55.4/5.09	84.3/6.09		
24	S-adenosylmethionine synthetase	0.86	0.90	1.67↑	28.40	6	416	43.8/4.96	43.0/5.65		
28	PREDICTED: alanine aminotransferase 2	1.25	1.49	1.96↑	37.40	4	367	53.6/6.78	57.9/7.85		
34	alpha-1,4-glucan-protein synthase	0.43↓	1.13	1.69↑	14.68	1	152	40.2/5.51	41.05/5.66		
35	PREDICTED: bifunctional aspartate aminotransferase and glutamate/aspartate-prephenate aminotransferase isoform X1	1.02	1.36	1.75↑	40.60	3	91	46.7/5.58	44.2/5.62		
50	glutathione S-transferase	1.45	1.56↑	1.52↑	34.23	7	318	19.75/4.92	25.40/6.84		

(continued on next page)

Table 2 (continued)

Spot ID	Protein name	Fold-change		SC (%)	M	Score	Mr/Pi	Organism	Accession No.					
		0.20												
Proteins involved in antioxidation and detoxification														
30	catalase/hydroperoxidase HPI(I)	1.21	1.42	1.68†	22.90	15	116	43.2/5.71	Alpha proteobacterium BAL					
33	12-oxophytidioate reductase 3	1.67†	1.71†	1.83†	46.7	17	82	49.6/6.56	Vitis vinifera					
37	PREDICTED: probable N-acetyl-gamma-glutamyl-phosphate reductase, chloroplastic	0.86	0.92	1.59†	56.33	13	54	44.1/5.99	Phoenix dactylifera					
42	ascorbate peroxidase	1.36	1.00	1.86†	35.22	5	376	38.1/4.52	Ziziphus jujube					
43	PREDICTED: L-ascorbate peroxidase 2, cytosolic	0.3†	1.12	1.78†	23.54	2	248	26.9/4.39	Vitis vinifera					
52	PREDICTED: 2-Cys peroxiredoxin BAS1, chloroplastic			new	72.64	2	79	29.7/5.55	Phoenix dactylifera					
53	PREDICTED: probable phospholipid hydroperoxide glutathione peroxidase XI			New	48.23	3	67	25.6/6.23	Cucumis melo					
Proteins involved in transcription regulation														
18	tex protein-related transcription accessory protein, putative	1.67†	1.65†	2.31†	33.16	8	142	44.7/4.85	Ricinus					
31	PREDICTED: DEAD-box ATP-dependent RNA helicase 56-like	1.29	0.76	1.59†	55.72	9	52	48.9/5.43	Vitis vinifera					
Proteins involved in protein synthesis, modification and degradation														
6	heat shock protein 101	2.90†	1.36	2.80†	22.85	4	560	94.6/5.2	Triticum turgidum subsp. durum					
32	mitochondrial translation elongation factor Tu	1.32	1.41	1.53†	17.94	2	371	46.4/5.96	Photophthora sojae					
2	PREDICTED: heat shock protein 83-like	2.20†	2.25†	2.50†	21.29	16	38	80.3/4.54	Photophthora sojae					
4	heat shock protein 70	2.10†	2.30†	2.20†	42.60	19	282	70.3/4.75	Gossypium hirsutum					
5	PREDICTED: stromal 70 kDa heat shock-related protein, chloroplastic-like	3.20†	3.41†	2.82†	34.31	5	191	70.4/4.85	Vitis vinifera					
7	heat shock protein	1.20	0.45†	1.30	21.56	2	419	70.6/5.12	Dicotylium fasciculatum					
8	HS70-like protein	1.98†	1.23	2.23†	28.95	7	72	75.0/5.30	Philodina roseola					
Proteins involved in protein synthesis, modification and degradation														
1	PREDICTED: ubiquitin carboxyl-terminal hydrolase 26	1.20	1.47	2.21†	44.97	6	372	109.8/4.42	119.8/5.77					
21	cysteine proteinase	1.86†	1.62†	2.13†	50.30	4	108	52.6/5.68	Elaeis guineensis					
47	PREDICTED: proteasome subunit beta type-7-B	1.45	1.68†	1.89†	28.57	1	75	28.9/4.42	Phoenix dactylifera					
36	chloroplast lipocalin proteins with other various functions	1.21	1.63†	1.74†	43.79	8	69	43.5/5.92	Ipomoea nil					
20	unnamed protein product													
29	PREDICTED: mucin-5AC-like	1.67†	1.71†	2.34†	13.14	1	271	52.1/5.32	Vitis vinifera					
51	hypothetical protein JCGZ_11042	1.47	1.32	1.64†	25.91	4	149	42.1/4.71	Astyanax mexicanus					
			New	23.02	3	63	30.6/6.42	Jatropha curcas						
							27.3/5.41							

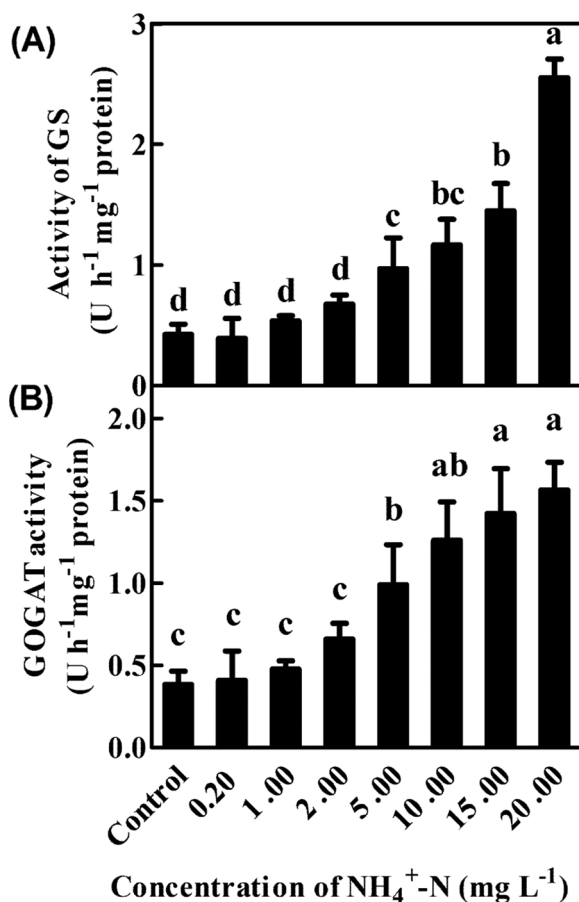


Fig. 8. Activities of GS (A) and GOGAT (B) in *H. verticillata* shoots exposed to different concentrations of $\text{NH}_4^+ \text{-N}$ for 5 days. For each parameter, different letters indicate significant difference among treatments according to the Tukey's HSD test ($p < 0.05$). Each bar indicates the mean \pm standard deviation ($n = 3$).

biosynthesis from $\text{NH}_4^+ \text{-N}$ consumes C-skeleton and energy from carbohydrates. However, excess $\text{NH}_4^+ \text{-N}$ inhibits photosynthetic activity in plants (Apudo et al., 2016; Britto and Kronzucker, 2002; Dendène et al., 1993). In eutrophic water bodies, the light availability for submersed plants were reduced during algal blooms, which limited the carbohydrates synthesis due to inefficient photosynthesis, thereby resulting in an imbalance of C-N metabolisms. Yuan et al. (2015) observed that high starch and soluble carbohydrates (SC) reserves in plants greatly contributed to $\text{NH}_4^+ \text{-N}$ uptake and assimilation. Elevated levels of HCO_3^- partially alleviated the submersed plant NH_4^+ toxicity, which might be due to the promotion of the SC synthesis and the decrease of the FAA/SC ratio (Dou et al., 2013). It was reported that decreased light availability and increased nutrient levels caused an increase in FAA and a decrease in SC, resulting in serious unbalance in C and N reserves in submersed plant *Potamogeton crispus* (Zhang et al., 2010). Similarly, in terms of N metabolism, the reduced photosynthetically active radiation exacerbated $\text{NH}_4^+ \text{-N}$ toxicity in two submersed plants (Cao et al., 2011). Under $\text{NH}_4^+ \text{-N}$ stress, the submersed macrophytes colonized at deep water were more efficient to maintain C-N metabolic balance than those grow at shallow water (Yuan et al., 2013). In this study, we found a significant increase in the activities of GS and GOGAT, which could be the requirement for $\text{NH}_4^+ \text{-N}$ detoxification. When challenged with excess $\text{NH}_4^+ \text{-N}$, cells would prefer to trigger the detoxification mechanism to remove $\text{NH}_4^+ \text{-N}$. Indeed, the GS-GOGAT cycle plays an important role to maintain the balance of carbon nitrogen in cells. Meanwhile, along with the activated GS-GOGAT cycle, a number of other enzymes may be increased as

a result of an elevated need for their respective relevant biological processes, as indicated by the enhanced abundance of proteins involved in carbohydrate metabolism, N assimilation and amino acid metabolism.

5. Conclusion

The present study provides new evidence of chloroplast ultrastructure and proteomics for the decline in photosynthesis and imbalance of carbon and nitrogen metabolisms in the aquatic macrophytes as a consequence of $\text{NH}_4^+ \text{-N}$ stress. Excess $\text{NH}_4^+ \text{-N}$ decreased the photosynthetic rate and the contents of soluble sugars, soluble proteins and chlorophyll, but increased the respiration rate, activities of GS and GOGAT and ROS accumulation in *H. verticillata*. Serious damage to chloroplast ultrastructure was observed, with disorganized lamellae and loose thylakoid membranes, which might in part explain the decrease of the photosynthesis rate of *H. verticillata*. Proteomic results showed that excess $\text{NH}_4^+ \text{-N}$ tended to decrease the abundance of six proteins involved in photosynthesis, but to increase the abundance of proteins involved in nitrogen assimilation and amino acid metabolism.

Author statement

Danlu Shi and Kai Zhuang: Conducting experiments, data analysis, writing-original draft preparation.

Yahua Chen and Fuli Xu: data analysis, interpreting results

Zhenguo Shen: Manuscript revision, project administration, funding acquisition, writing - review & editing.

Zhubing Hu: Writing - review & editing.

Declaration of Competing Interest

The authors report no declarations of interest.

Acknowledgments

This study was financially supported by the National Natural Science Foundations of China (41030529); Innovative Scientific and Technological Talents in Henan Province (20HASTIT041 to Z.H.) and the 111 Project#D16014.

Appendix A. Supplementary data

Supplementary material related to this article can be found, in the online version, at doi:<https://doi.org/10.1016/j.aquatox.2020.105585>.

References

- Abu Bakar, A.F., Yusoff, I., Fatt, N.T., Othman, F., Ashraf, M.A., 2013. Arsenic, zinc, and aluminium removal from gold mine wastewater effluents and accumulation by submerged aquatic plants (*Cabomba piauhyensis*, *Egeria densa*, and *Hydrilla verticillata*). *Biomed Res. Int.* 2013 <https://doi.org/10.1155/2013/890803>. 890803-890803.
- Apudo, A.A., Cao, Y., Wakibia, J., Li, W., Liu, F., 2016. Physiological plastic responses to acute $\text{NH}_4^+ \text{-N}$ toxicity in *Myriophyllum spicatum* L. cultured in high and low nutrient conditions. *Environ. Exp. Bot.* 130, 79–85. <https://doi.org/10.1016/j.envexpbot.2016.05.009>.
- Bai, L., Ma, X.N., Zhang, G.Z., Song, S.F., Zhou, Y., Gao, L.J., Miao, Y.C., Song, C.P., 2014. A receptor-like kinase mediates ammonium homeostasis and is important for the polar growth of root hairs in *Arabidopsis*. *Plant Cell* 26, 1497–1511. <https://doi.org/10.1105/tpc.114.124586>.
- Bakker, E.S., Wood, K.A., Pagès, J.F., (Ciska) Veen, G.F., Christianen, M.J.A., Santamaría, L., Nollet, B.A., Hilt, S., 2016. Herbivory on freshwater and marine macrophytes: A review and perspective. *Aquat. Bot.* 135, 18–36. <https://doi.org/10.1016/j.aquabot.2016.04.008>.
- Banks, F.M., Driscoll, S.P., Parry, M.A.J., Lawlor, D.W., Knight, J.S., Gray, J.C., Paul, M.J., 1999. Decrease in phosphoribulokinase activity by antisense RNA in transgenic Tobacco. Relationship between photosynthesis, growth, and allocation at different nitrogen levels. *Plant Physiol.* 119, 1125–1136. <https://doi.org/10.1104/pp.119.3.1125>.
- Berteli, F., Corrales, E., Guerrero, C., Ariza, M.J., Pliego, F., Valpuesta, V., 1995. Salt stress increases ferredoxin-dependent glutamate synthase activity and protein level in

- the leaves of tomato. *Physiol. Plant.* 93, 259–264. <https://doi.org/10.1111/j.1399-3054.1995.tb02226.x>.
- Bhagowati, B., Ahamad, K.U., 2019. A review on lake eutrophication dynamics and recent developments in lake modeling. *Ecohydrol. Hydrobiol.* 19, 155–166. <https://doi.org/10.1016/j.ecohyd.2018.03.002>.
- Bornette, G., Puijalon, S., 2011. Response of aquatic plants to abiotic factors: a review. *Aquat. Sci.* 73, 1–14. <https://doi.org/10.1007/s00027-010-0162-7>.
- Bradford, M.M., 1976. A rapid and sensitive method for the quantitation of microgram quantities of protein utilizing the principle of protein-dye binding. *Anal. Biochem.* 72, 248–254. [https://doi.org/10.1016/0003-2697\(76\)90527-3](https://doi.org/10.1016/0003-2697(76)90527-3).
- Britto, D.T., Kronzucker, H.J., 2002. NH_4^+ toxicity in higher plants: a critical review. *J. Plant Physiol.* 159, 567–584. <https://doi.org/10.1078/0176-1617-0774>.
- Britto, D.T., Siddiqi, Y., Glass, A.D.M., Kronzucker, H.J., 2001. Futile transmembrane NH_4^+ cycling: a cellular hypothesis to explain ammonium toxicity in plants. *Proc. Natl. Acad. Sci. U. S. A.* v. 98, 4255–4258. <https://doi.org/10.1073/pnas.061034698>.
- Cao, T., Ni, L.Y., Xie, P., 2004. Acute biochemical responses of a submersed macrophyte, *Potamogeton crispus* L., to high ammonium in an aquarium experiment. *J. Freshw. Ecol.* 19, 279–284. <https://doi.org/10.1080/02705060.2004.9664542>.
- Cao, T., Ni, L.Y., Xie, P., Xu, J., Zhang, M., 2011. Effects of moderate ammonium enrichment on three submersed macrophytes under contrasting light availability. *Freshw. Biol.* 56, 1620–1629. <https://doi.org/10.1111/j.1365-2427.2011.02601.x>.
- Chen, F.Z., Song, X.L., Hu, Y.H., Liu, Z.W., Qin, B.Q., 2009. Water quality improvement and phytoplankton response in the drinking water source in Meiliang Bay of Lake Taihu, China. *Ecol. Eng.* 35, 1637–1645. <https://doi.org/10.1016/j.ecoleng.2008.01.001>.
- Dendène, M.A., Rolland, T., Trémolières, M., Carbiener, R., 1993. Effect of ammonium ions on the net photosynthesis of three species of *Elodea*. *Aquat. Bot.* 46, 301–315. [https://doi.org/10.1016/0304-3770\(93\)90010-T](https://doi.org/10.1016/0304-3770(93)90010-T).
- Dou, Y.Y., Wang, B.Z., Chen, L.Y., Yin, D.Q., 2013. Alleviating versus stimulating effects of bicarbonate on the growth of *Vallisneria natans* under ammonia stress. *Environ. Sci. Pollut. Res. Int.* v. 20, 5281–5288. <https://doi.org/10.1007/s11356-013-1514-3>.
- Gomes, M.P., Le Manac'h, S.G., Maccario, S., Labrecque, M., Lucotte, M., Juneau, P., 2016. Differential effects of glyphosate and aminomethylphosphonic acid (AMPA) on photosynthesis and chlorophyll metabolism in willow plants. *Pest. Biochem. Physiol.* 130, 65–70. <https://doi.org/10.1016/j.pestbp.2015.11.010>.
- Gough, S.P., Kannangara, C.G., von Wettstein, D., 1993. Glutamate 1-Semialdehyde aminotransferase as a target for herbicides. In: Böger, P., Sandman, G. (Eds.), *Target assays for modern herbicides and related phytotoxic compounds*. Lewis Publishers, Boca Raton, pp. 21–27.
- Hazen, S.P., Wu, Y., Kreps, J.A., 2003. Gene expression profiling of plant responses to abiotic stress. *Funct. Integr. Genomic.* 3, 105–111. <https://doi.org/10.1007/s10142-003-0088-4>.
- He, Y., Rui, H.Y., Chen, C., Chen, Y.H., Shen, Z.G., 2016. The role of roots in the accumulation and removal of cadmium by the aquatic plant *Hydrilla verticillata*. *Environ. Sci. Pollut. Res. Int.* 23, 13308–13316. <https://doi.org/10.1007/s11356-016-6505-8>.
- Heide, H., Kalisz, H.M., Follmann, H., 2004. The oxygen evolving enhancer protein 1 (OEE) of photosystem II in green algae exhibits thioredoxin activity. *J. Plant Physiol.* 161, 139–149. <https://doi.org/10.1078/0176-1617-01033>.
- Henkes, S., Sonnewald, U., Badur, R., Flachmann, R., Stitt, M., 2001. A small decrease of plastid transketolase activity in antisense tobacco transformants has dramatic effects on photosynthesis and phenylpropanoid metabolism. *Plant Cell* 13, 535. <https://doi.org/10.1105/tpc.13.3.535>.
- Horn, R., Grundmann, G., Paulsen, H., 2007. Consecutive binding of chlorophylls a and b during the assembly *in vitro* of light-harvesting chlorophyll-a/b Protein (LHCIIb). *J. Mol. Biol.* 366, 1045–1054. <https://doi.org/10.1016/j.jmb.2006.11.069>.
- Horn, R., Paulsen, H., 2002. Folding *in vitro* of light-harvesting chlorophyll a/b protein is coupled with pigment binding. *J. Mol. Biol.* 318, 547–556. [https://doi.org/10.1016/S0022-2836\(02\)00115-8](https://doi.org/10.1016/S0022-2836(02)00115-8).
- Huang, M.J., Fang, Y., Xiao, Y., Sun, J.L., Jin, Y.L., Tao, X., Ma, X.R., He, K.Z., Zhao, H., 2014. Proteomic analysis to investigate the high starch accumulation of duckweed (*Lemna punctata*) under nutrient starvation. *Ind. Crop. Prod.* 59, 299–308. <https://doi.org/10.1016/j.indcrop.2014.05.029>.
- Jain, M.S., Kalamdhad, A.S., 2018. A review on management of *Hydrilla verticillata* and its utilization as potential nitrogen-rich biomass for compost or biogas production. *Bioresour. Technol. Reports* 1, 69–78. <https://doi.org/10.1016/j.biteb.2018.03.001>.
- Jiang, J.G., Shen, Y.F., 2007. Development of the microbial communities in lake donghu in relation to water quality. *Environ. Monit. Assess.* 127, 227–236. <https://doi.org/10.1007/s10661-006-9275-9>.
- Jorrín, J.V., Rubiales, D., Dumas-Gaudot, E., Recorbet, G., Maldonado, A., Castillejo, M.A., Curto, M., 2006. Proteomics: a promising approach to study biotic interaction in legumes. A review. *Euphytica* 147, 37–47. <https://doi.org/10.1007/s10681-006-3061-1>.
- Kaszycki, P., Dubicka-Lisowska, A., Augustynowicz, J., Piwowarczyk, B., Wesołowski, W., 2018. *Callitrichia cophocarpa* (water starwort) proteome under chromate stress: evidence for induction of a quinone reductase. *Environ. Sci. Pollut. Res.* 25, 8928–8942. <https://doi.org/10.1007/s11356-017-1067-y>.
- Kautsky, H., 1991. Influence of eutrophication on the distribution of phylobenthic plant and animal communities. *Int. Rev. Hydrobiol.* 76, 423–432. <https://doi.org/10.1002/iroh.19910760315>.
- Kieselbach, T., Hagman, Andersson, B., Schröder, W., 1998. The thylakoid lumen of chloroplasts. Isolation and characterization. *J. Biol. Chem.* 273, 6710–6716. <https://doi.org/10.1074/jbc.273.12.6710>.
- Kim, E.Y., Choi, Y.H., Lee, J.I., Kim, I.H., Nam, T.J., 2015. Antioxidant activity of oxygen evolving enhancer protein 1 purified from *Caposiphon fulvescens*. *J. Food Sci.* 80, H1412–H1417. <https://doi.org/10.1111/1750-3841.12883>.
- Kosová, K., Vítámvás, P., Prášil, I.T., Renaut, J., 2011. Plant proteome changes under abiotic stress — Contribution of proteomics studies to understanding plant stress response. *J. Proteomics* 74, 1301–1322. <https://doi.org/10.1016/j.jprot.2011.02.006>.
- Larras, F., Regier, N., Planchon, S., Poté, J., Renaut, J., Cosio, C., 2013. Physiological and proteomic changes suggest an important role of cell walls in the high tolerance to metals of *Elodea nuttallii*. *J. Hazard. Mater.* 263, 575–583. <https://doi.org/10.1016/j.jhazmat.2013.10.016>.
- Lewis, M., Pryor, R., 2013. Toxicities of oils, dispersants and dispersed oils to algae and aquatic plants: Review and database value to resource sustainability. *Environ. Pollut.* 180, 345–367. <https://doi.org/10.1016/j.envpol.2013.05.001>.
- Li, X., Xi, H.C., Sun, X.D., Yang, Y.Q., Yang, S.H., Zhou, Y.L., Zhou, X.M., Yang, Y.P., 2015. Comparative proteomics exploring the molecular mechanism of eutrophic water purification using water hyacinth (*Eichhornia crassipes*). *Environ. Sci. Pollut. Res. Int.* 22, 8643–8658. <https://doi.org/10.1007/s11356-014-4020-3>.
- Lin, A.P., Wang, C., Qiao, H.J., Pan, G.H., Wang, G.C., Song, L.Y., Wang, Z.Y., Sun, S., Zhou, B.C., 2009. Study on the photosynthetic performances of Enteromorpha prolifera collected from the surface and bottom of the sea of Qingdao sea area. *Chin. Sci. Bull.* 54, 399–404. <https://doi.org/10.1007/s11434-009-0025-6>.
- Longworth, J., Wu, D.Y., Huete-Ortega, M., Wright, P.C., Vaidyanathan, S., 2016. Proteome response of *Phaeodactylum tricornutum*, during lipid accumulation induced by nitrogen depletion. *Algal Res.* v. 18, 213–224. <https://doi.org/10.1016/j.algal.2016.06.015>.
- Loreto, F., Velikova, V., 2001. Isoprene produced by leaves protects the photosynthetic apparatus against ozone damage, quenches ozone products, and reduces lipid peroxidation of cellular membranes. *Plant Physiol.* 127, 1781. <https://doi.org/10.1104/pp.010497>.
- Ma, X.X., Wang, L.C., Wu, H., Li, N., Ma, L., Zeng, C.F., Zhou, Y., Yang, J., 2015. Impact of Yangtze River Water Transfer on the Water Quality of the Lixia River Watershed. *China.* PLOS ONE 10, e0119720. <https://doi.org/10.1371/journal.pone.0119720>.
- Marmagno, A., Salvi, D., Rolland, N., Ephrithikhine, G., Joyard, J., Barbier-Brygoo, H., 2006. Purification and fractionation of membranes for proteomic analyses. In: salinas, J., Sanchez-Serrano, J.J. (Eds.), *Arabidopsis Protocols*. Humana Press, Totowa, NJ, pp. 403–420. <https://doi.org/10.1385/1-59745-003-0:403>.
- Mayfield, S.P., Rahire, M., Frank, G., Zuber, H., Rochaix, J.D., 1987. Expression of the nuclear gene encoding oxygen-evolving enhancer protein 2 is required for high levels of photosynthetic oxygen evolution in *Chlamydomonas reinhardtii*. *Proc. Natl. Acad. Sci. U. S. A.* 84, 749–753. <https://doi.org/10.1073/pnas.84.3.749>.
- Molas, J., 1998. Changes in morphological and anatomical structure of cabbage (*Brassica oleracea* L.) outer leaves and in ultrastructure of their chloroplasts caused by an in vitro excess of nickel. *Photosynthetica* 34, 513–522. <https://doi.org/10.1023/A:1006805327340>.
- Navari-Izzo, F., Pinzino, C., Quartacci, M., Sgherri, C., 1999. Superoxide and hydroxyl radical generation, and superoxide dismutase in PSII membrane fragments from wheat. *Free Radic. Res.* 31 (Suppl), S3–9. <https://doi.org/10.1080/10715769900301251>.
- Panda, S.K., Khan, M.H., 2004. Changes in growth and superoxide dismutase activity in *Hydrilla verticillata* L. under abiotic stress. *Braz. J. Plant Physiol.* 16, 115–118. <https://doi.org/10.1590/S1677-04202004000200007>.
- Park, S., Kang, D., Kim, Y., Lee, S.M., Chung, Y., Sung, K., 2011. Biosorption and growth inhibition of wetland plants in water contaminated with a mixture of arsenic and heavy metals. *Eng. Life Sci.* 11, 84–93. <https://doi.org/10.1002/elsc.20100024>.
- Piwpuan, N., Jampeetong, A., Brix, H., 2014. Ammonium tolerance and toxicity of *Actinostirus grossus* - A candidate species for use in tropical constructed wetland systems. *Ecotox. Environ. Safe.* 107, 319–328. <https://doi.org/10.1016/j.ecoenv.2014.05.032>.
- Puritch, G.S., Barker, A.V., 1967. Structure and function of tomato leaf chloroplasts during ammonium toxicity. *Plant Physiol.* 42, 1229. <https://doi.org/10.1104/pp.42.91229>.
- Rodziewicz, P., Swarcewicz, B., Chmielewska, K., Wojakowska, A., Stobiecki, M., 2014. Influence of abiotic stresses on plant proteome and metabolome changes. *Acta Physiol.* 36. <https://doi.org/10.1007/s11738-013-1402-y>.
- Saunkaew, P., Wangpakapattanawong, P., Jampeetong, A., 2011. Growth, morphology, ammonium uptake and nutrient allocation of *Myriophyllum brasiliense* Cambess. under high NH_4^+ concentrations. *Ecotoxicology* 20 (2011). <https://doi.org/10.1007/s10646-011-0744-8>.
- Shi, D.L., Zhuang, K., Xia, Y., Zhu, C.H., Chen, C., Hu, Z.B., Shen, Z.G., 2017. *Hydrilla verticillata* employs two different ways to affect DNA methylation under excess copper stress. *Aquat. Toxicol.* 193, 97–104. <https://doi.org/10.1016/j.aquatox.2017.10.007>.
- Singh, P., Kumar, P.A., Abrol, Y.P., Naik, M.S., 1986. Photorespiratory nitrogen cycle - A critical evaluation. *Physiol. Plant.* 66, 169–176. <https://doi.org/10.1111/j.1399-3054.1986.tb01252.x>.
- Srivastava, S., Bhainsa, K.C., D'Souza, S.F., 2010. Investigation of uranium accumulation potential and biochemical responses of an aquatic weed *Hydrilla verticillata* (L.f.) Royle. *Bioresour. Technol.* 101, 2573–2579. <https://doi.org/10.1016/j.biortech.2009.10.054>.
- Srivastava, S., D'Souza, S.F., 2009. Increasing sulfur supply enhances tolerance to arsenic and its accumulation in *Hydrilla verticillata* (L.f.) Royle. *Environ. Sci. Technol.* 43, 6308–6313. <https://doi.org/10.1021/es900304x>.
- Srivastava, S., Mishra, S., Tripathi, R.D., Dwivedi, S., Gupta, D.K., 2006. Copper-induced oxidative stress and responses of antioxidants and phytochelatins in *Hydrilla verticillata* (L.f.) Royle. *Aquat. Toxicol.* 80, 405–415. <https://doi.org/10.1016/j.aquatox.2006.10.006>.
- Stenbaek, A., Jensen, P.E., 2010. Redox regulation of chlorophyll biosynthesis. *Phytochemistry* 71, 853–859. <https://doi.org/10.1016/j.phytochem.2010.03.022>.
- Su, S.Q., Zhou, Y., Qin, J.G., Wang, W., Yao, W., Song, L., 2012. Physiological responses of *Egeria densa* to high ammonium concentration and nitrogen deficiency.

- Chemosphere 86, 538–545. <https://doi.org/10.1016/j.chemosphere.2011.10.036>.
- Thagela, P., Yadav, R.K., Mishra, V., Dahuja, A., Ahmad, A., Singh, P.K., Tiwari, B.S., Abraham, G., 2017. Salinity-induced inhibition of growth in the aquatic pteridophyte *Azolla microphylla* primarily involves inhibition of photosynthetic components and signaling molecules as revealed by proteome analysis. *Protoplasma* 254, 303–313. <https://doi.org/10.1007/s00709-016-0946-2>.
- Wang, C., Zhang, S.H., Wang, P.F., Li, W., Lu, J., 2010. Effects of ammonium on the antioxidative response in *Hydrilla verticillata* (L.f.) Royle plants. *Ecotox. Environ. Safe.* 73, 189–195. <https://doi.org/10.1016/j.ecoenv.2009.08.012>.
- Wang, Y.S., Luo, Z.S., Du, R.X., 2015. Nitric oxide delays chlorophyll degradation and enhances antioxidant activity in banana fruits after cold storage. *Acta Physiol. Plant.* v. 37<https://doi.org/10.1007/s11738-015-1821-z>. 1821–1821.
- Weisse, T., 2008. Limnecology: The Ecology of Lakes and Streams. *J. Plankton Res.* 30, 489–490. <https://doi.org/10.1093/plankt/fbn013>.
- Wilson, A.T., Calvin, M., 1955. The photosynthetic cycle. CO₂ dependent transients. *J. Am. Chem. Soc.* 77, 5948–5957. <https://doi.org/10.1021/ja01627a050>.
- Xue, P.Y., Li, G.X., Liu, W.J., Yan, C.Z., 2010. Copper uptake and translocation in a submerged aquatic plant *Hydrilla verticillata* (L.f.) Royle. *Chemosphere* 81, 1098–1103. <https://doi.org/10.1016/j.chemosphere.2010.09.023>.
- Yamamoto, K., Godowski, P., Picard, D., 1988. Ligand-regulated nonspecific inactivation of receptor function: a versatile mechanism for signal transduction. *Cold Spring Harb. Symp. Quant. Biol.* 53 (Pt 2), 803–811. <https://doi.org/10.1101/sqb.1988.053.01.091>.
- Yemm, E.W., Willis, A.J., 1954. The estimation of carbohydrates in plant extracts by anthrone. *Biochem. J.* 57, 508–514. <https://doi.org/10.1042/bj0570508>.
- Yin, X.L., Zhang, J., Guo, Y.Y., Fan, J.L., Hu, Z., 2016. Physiological responses of *Potamogeton crispus* to different levels of ammonia nitrogen in constructed wetland. *Water Air Soil Pollut.* v. 227 <https://doi.org/10.1007/s11270-016-2763-9>. 65–65.
- Yuan, G.X., Cao, T., Fu, H., Ni, L.Y., Zhang, X.L., Li, W., Song, X., Xie, P., Jeppesen, E., 2013. Linking carbon and nitrogen metabolism to depth distribution of submersed macrophytes using high ammonium dosing tests and a lake survey. *Freshw. Biol.* 58, 2532–2540. <https://doi.org/10.1111/fwb.12230>.
- Yuan, G.X., Fu, H., Li, W., Zhong, J.Y., Feng, Q., Ni, L.Y., Xie, P., Cao, T., Guo, C.J., Lou, Q., 2017. The C/N metabolic responses to water depth gradients and seasons in natural macrophyte populations. *Ecol. Eng.* 104, 195–204. <https://doi.org/10.1016/j.ecoleng.2017.04.003>.
- Yuan, G.X., Fu, H., Zhong, J.Y., Cao, T., Ni, L.Y., Zhu, T.S., Li, W., Song, X., 2015. Nitrogen/carbon metabolism in response to NH₄⁺ pulse for two submersed macrophytes. *Aquat. Bot.* 121, 76–82. <https://doi.org/10.1016/j.aquabot.2014.12.001>.
- Zaefyzadeh, M., Quliyev, R.A., Babayeva, S.M., Abbasov, M.A., 2009. The effect of the interaction between genotypes and drought stress on the superoxide dismutase and chlorophyll content in durum wheat landraces. *Turk. J. Biol.* 33, 1–7. <http://journals.tubitak.gov.tr/biology/issues/biy-09-33-1/biy-33-1-1-0801-12.pdf>.
- Zhang, M., Cao, T., Ni, L.Y., Xie, P., Li, Z.Q., 2010. Carbon, nitrogen and antioxidant enzyme responses of *Potamogeton crispus* to both low light and high nutrient stresses. *Environ. Exp. Bot.* 68, 44–50. <https://doi.org/10.1016/j.enexpbot.2009.09.003>.
- Zhang, X.F., Liu, Z.W., 2011. Interspecific competition effects on phosphorus accumulation by *Hydrilla verticillata* and *Vallisneria natans*. *J. Environ. Sci.* 23, 1274–1278. [https://doi.org/10.1016/S1001-0742\(10\)60548-7](https://doi.org/10.1016/S1001-0742(10)60548-7).
- Zhong, A.W., Cao, T., Ni, L.Y., Xie, P., 2013. Growth and membrane permeability of two submersed macrophytes in response to ammonium enrichment. *Aquat. Biol.* 19, 55–64. <https://doi.org/10.3354/ab00514>.
- Zhou, X.H., He, Z.L., Jones, K.D., Li, L.G., Stoffella, P.J., 2017. Dominating aquatic macrophytes for the removal of nutrients from waterways of the Indian river lagoon basin, south Florida, USA. *Ecol. Eng.* 101, 107–119. <https://doi.org/10.1016/j.ecoleng.2017.01.006>.
- Zhou, Y., Bai, L., Song, C.P., 2015. Ammonium homeostasis and signaling in plant cells. *Sci. Bull.* 60, 741–747. <https://doi.org/10.1007/s11434-015-0759-2>.
- Zhuang, K., Shi, D.L., Hu, Z.B., Xu, F.L., Chen, Y.H., Shen, Z.G., 2019. Subcellular accumulation and source of O₂^{·-} and H₂O₂ in submerged plant *Hydrilla verticillata* (L.f.) Royle under NH₄⁺-N stress condition. *Aquat. Toxicol.* 207, 1–12. <https://doi.org/10.1016/j.aquatox.2018.11.011>.